Scientific Research Publishing

Journal of High Energy Physics, Gravitation and Cosmology, 2024, 10, 149-157
https://www.scirp.org/journal/jhepgc
ISSN Online: 2380-4335
ISSN Print: 2380-4327

The Formation of Oscillation Patterns Based on the Planetary Gravitational Field and Their Suitability for Earthquake Prediction

Michael E. Nitsche

Z & S Institut, Grosselfingen, Germany
Email: michael.nitsche@lettris.de

How to cite this paper: Nitsche, M.E. (2024) The Formation of Oscillation Patterns Based on the Planetary Gravitational Field and Their Suitability for Earthquake Prediction. *Journal of High Energy Physics, Gravitation and Cosmology*, **10**, 149-157.
https://doi.org/10.4236/jhepgc.2024.101013

Received: September 4, 2023
Accepted: January 14, 2024
Published: January 17, 2024

Abstract

The fluctuating planetary gravitational field influences not only activities on the Sun but also on the Earth. A special correlation function describes the harmonics of these fluctuations. Groups of earthquakes form oscillation patterns that differ significantly from randomly chosen control groups. These patterns are suitable as an element of an AI for the probability of earthquakes.

Keywords

Planetary Gravitational Field, Earthquake Prediction, AI

1. Introduction

In a study of the nonlinear interaction of the fluctuating planetary gravitational field with the lithosphere suggests that not only the directly acting gravitational forces are of influence, but mainly higher harmonics of the celestial bodies considered as oscillators on large scales [1] [2]. In the meantime, resonances caused by fluctuating gravitation can also be detected on small scales in the laboratory [3].

The kinematics of the planets corresponds to oscillators, which were stable over billions of years in evolution and were able to unfold their effects. The gravitational forces are weak and sensually directly perceptible only in the coupling of sun and moon in the tides.

Tidal stresses are very small, so there is still a lot of debate about whether they can even trigger an earthquake. Several studies have found no correlation between tides and earthquake occurrence, e.g. Kennedy *et al.*, 2004 [4]. Other studies report small positive correlations, e.g., Kasahara, 2002 [5]. Some recent re-

search by Metivier *et al.* (2009) suggests evidence that tidal-induced uplift may reduce the normal stresses that hold faults together [6].

Previous studies related to earthquake triggering do not take into account planetary gravitational interactions, e.g. [7] [8] [9].

The special effects of the fluctuating gravitational field become visible only in the harmonics. A correlation function constructed to indicate that the change in probabilities for stable (harmonic) and unstable (discordant) states is also applied to earthquake triggering [10] [11].

As shown in previous publications [1] [12] [13], characteristic oscillation patterns can be found for groups of earthquakes that differ significantly from randomly chosen control groups. In [9] it was proposed to use these oscillation patterns similar to an AI as an element for earthquake prediction. Initial research published here confirms this method.

A correlation function (derivation of the function see [1] [2]) is a Fourier series expansion of a periodic process and can be optimized both in its order and in its frequencies for the respective problem. It has the function of a high-pass filter (**Figure 1**).

The calculation of the harmonics of the planetary gravitational field results in a matrix in which each element in turn consists of the superposition of several oscillations. These oscillation patterns of the individual earthquakes can in turn be superimposed and form the characteristics of this group. If these groups, characteristics are compared with very many randomly selected comparison groups, it is possible to assess whether the group of earthquakes differs significantly from the expected values.

For the group of 41 strongest earthquakes of the last century (1900-2000), this pattern for the matrix of harmonicity looks as follows (data of earthquakes in [1]).

Computer printout of the 41 earthquakes to supplement **Figure 2**.

```
Statistics 4: Probability of events: correlation matrix H
 Order of the correlation: 3 ; time shift d: 0 h: 0;
 GROUP-MEMBERS: 41 ; NUMBER OF THE GROUPS: 10000
 Julian-date-start: 2415019.458333 Julian-date-end: 2488068.458345
 Accidental selection;  TEST: Number of accidental selection >= correlation


Matrix H of the probability of error:
1       2       3       4       5       6       7       8       9      10

  1       *      87.89   14.43   36.86   56.76   46.31   22.17   85.17   51.60   76.43 PR  77.14
  2      87.89    *      33.85    5.72   42.69   28.65   10.65   83.11   93.97    6.73 PR  27.85
  3      14.43   33.85    *      68.44   13.49   39.08   38.94   70.76   53.72   61.18 PR  35.47
  4      36.86    5.72   68.44    *      26.73   59.78   46.11   70.55   81.44   76.33 PR  54.01
  5      56.76   42.69   13.49   26.73    *       0.03   95.06   57.33   99.98   63.99 PR  66.29
  6      46.31   28.65   39.08   59.78    0.03    *      50.46   71.96   90.05    0.19 PR   4.37
  7      22.17   10.65   38.94   46.11   95.06   50.46    *      69.11   26.17   51.78 PR  39.23
  8      85.17   83.11   70.76   70.55   57.33   71.96   69.11    *      60.60   65.81 PR  94.42
  9      51.60   93.97   53.72   81.44   99.98   90.05   26.17   60.60    *      42.53 PR  98.73
 10      76.43    6.73   61.18   76.33   63.99    0.19   51.78   65.81   42.53    *    PR  23.51
bigger are:   63.62 %
 1=SUN;  2=MOON;  3=MERKUR;  4=VENUS;  5=MARS;  6=JUPITER;  7=SATURN;  8=URANUS;  9=NEPTUN; 10=PLUTO;
 BEGIN: year: 1900 month: 1 day: 1 hour: 0  END: year: 2100 month: 1 day: 1 hour: 0
```

$$H_{i,j} = \sum_{s=1}^{N\cdot 12-1} a_k \cos(s\cdot\alpha); mit(k = s \bmod 12)$$
$$a_k = \{0,1,-2,3,-5,0,3,0,-5,3,-2,1\} \quad (1)$$

Figure 1. $H_{i,j}$ is the correlation of two celestial bodies; α is the angle between two celestial bodies; a_k are the 12 coefficients of the Fourier series repeated N times; N is the order of the correlation function. The coefficients a_k were obtained from a Fourier transform describing the change in probability for stable and unstable processes, respectively.

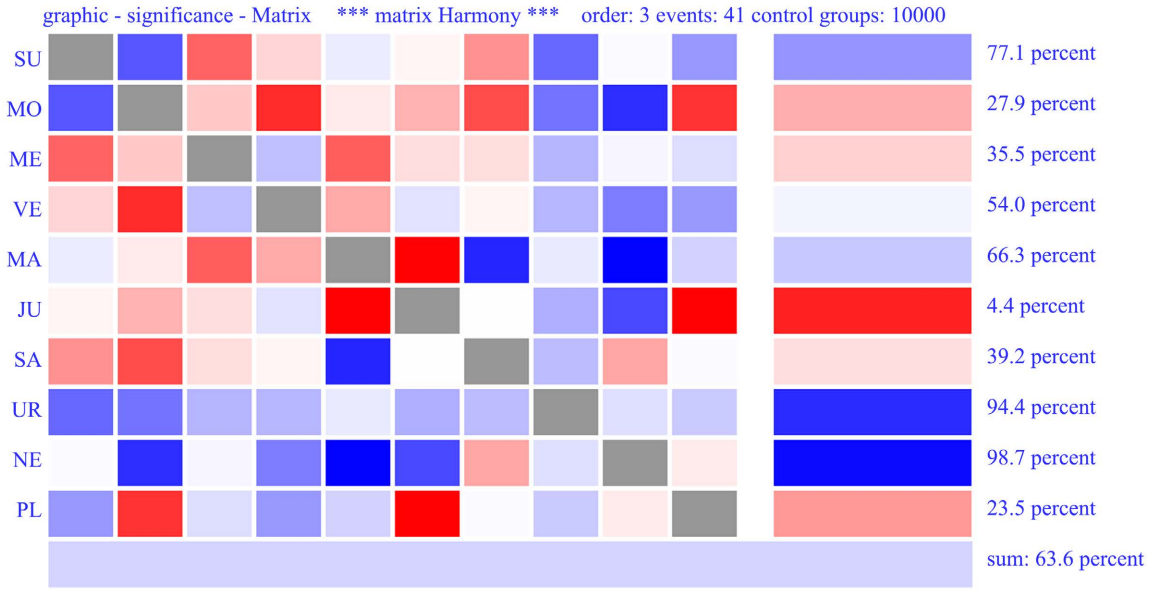

Figure 2. The figure shows the deviations of the pattern "Harmony H" ($H_{i,j}$) from the expected values for the individual correlations. On the right side of the figure the row sums (planets) are shown. The lower bar indicates the value for the entire matrix. Blue are disharmonies, red are harmonies. A strong color indicates a strong deviation from the statistical mean. In this example, the disharmonic correlation of Jupiter has the value of 4.4% (that means only 4.4% of the control groups have a higher harmony). In contrast, Neptune is significantly disharmonic with 98.7% (98.7% of the control groups have a higher harmony).

Although this matrix already represents a pattern, not all characteristics of the group of earthquakes are yet captured. Since it is a wave function, the energy is also a characteristic (**Figure 3**).

The investigations have shown that the matrices harmony $H_{i,j}$ and energy $I_{i,j}$, supplemented by the matrices of the 1st derivative of the correlation function dynamics $D_{i,j}$ and dynamics absolute $DA_{i,j}$ determine the pattern formation.

An evaluation of time with respect to the probability of an earthquake is composed of the pattern elements listed above. For the matrix the correlation function as given by Linfoot for the object-image comparison is suitable. (Linfoot criteria: fidelity, correlation, relative structure content.)

The total value of a matrix is currently compared with the value of the pattern.

$$\text{Probability} = a_1 * H_{i,j} + a_2 * I_{i,j} + a_3 * D_{i,j} + a_4 * DA_{i,j} \quad (2)$$

The coefficients a_i are determined according to an optimization procedure. Here, the coefficients a_i indicate the significance of the matrices for the examined

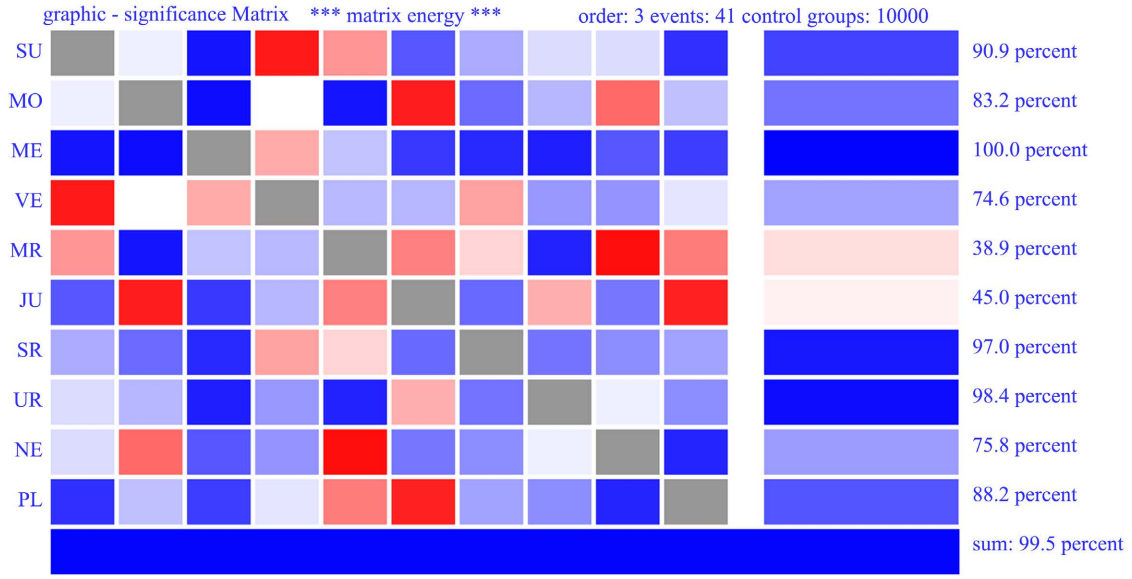

Figure 3. The figure shows the deviations of the pattern "Energy I" from the expected values for the individual correlations. On the right side of the figure, the row sums (planets) are shown. The lower bar indicates the value for the entire matrix. Blue indicates weak energies, red indicates strong energies. A strong color indicates a strong deviation from the statistical mean. In this example, the correlation of Saturn has the value of 97.8% (that means 97.8% of the control groups have a higher energy).

group of events. If the harmony or disharmony is significant for a group, then the matrix $H_{i,j}$ will be weighted particularly strongly.

The following assignment applies:

$H_{i,j}$, for the harmony and disharmony.

$I_{i,j}$, for the absolute value (energy) of the superimposed waves.

$D_{i,j}$, for the velocity of the change of the oscillation state (1st derivative).

$DA_{i,j}$, for the acceleration (force) of the velocity change.

For earthquakes, the optimization objective is the distance from the continuum. The pattern must detect as many earthquakes as possible from a list of earthquakes and at the same time identify few events from a random list as earthquakes (discriminatory power). Gradient methods are not suitable for the optimization process because it is not a continuous objective function.

The pattern used here finds 100% from the list of 41 strongest earthquakes. However, it also identifies 25.8% of the events as earthquakes from a randomly selected list. The discriminatory power (difference) from the continuum is 74.2.

41 strong earthquakes in a century are not very many compared to the many earthquakes that also still occur, albeit weaker and with less personal injury. Therefore, it is not expected that the probability of a strong earthquake will have local maxima only slightly above the number 41 in 100 years.

The time environment to the 1st earthquake from the list of 41 can be seen in Figure 4.

Earthquakes, as the investigations show, take place in a characteristic temporal environment, which often starts with foreshocks. Therefore, it seems to make sense to include the temporal environment in the considerations (Figure 5).

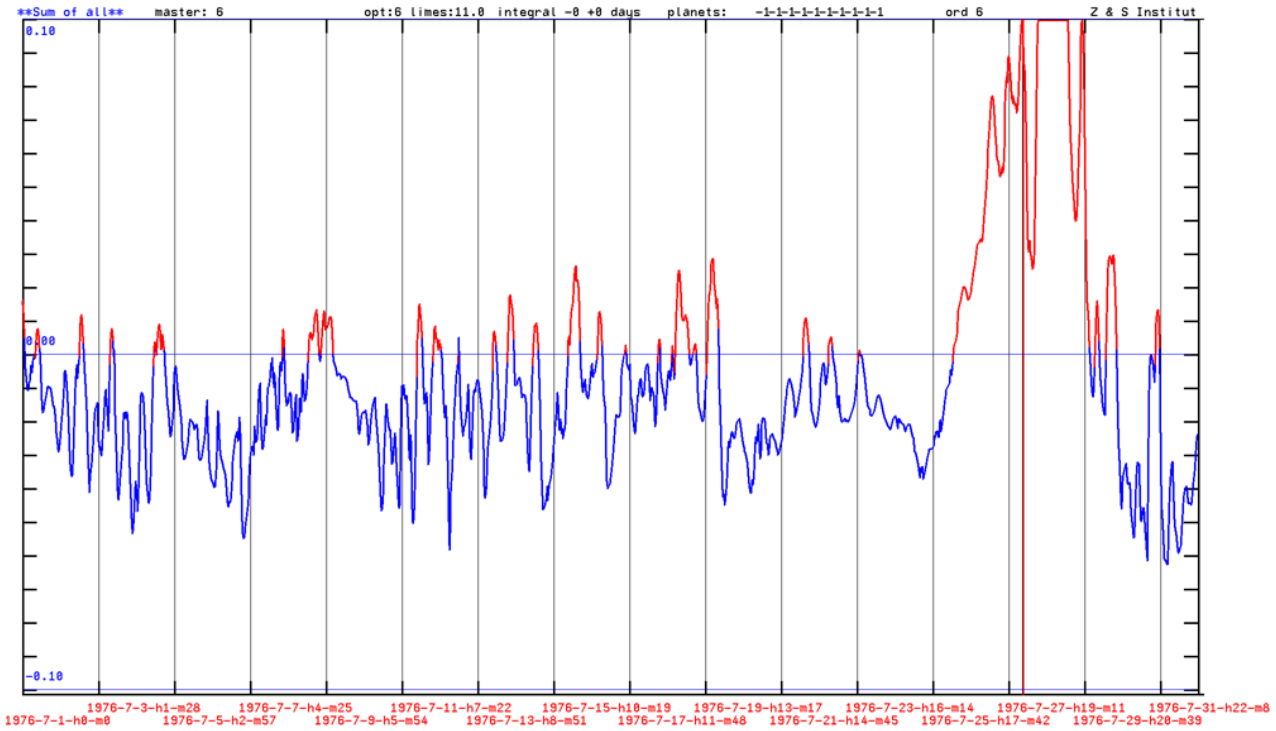

Figure 4. The month of the first earthquake (China; Tangshan; 28.7.1976; 03:42:00) from the list of 41 earthquakes. The time of the earthquake is indicated by the vertical red line. The curve indicates the change in the probability of an earthquake according to the pattern of the 41 earthquakes.

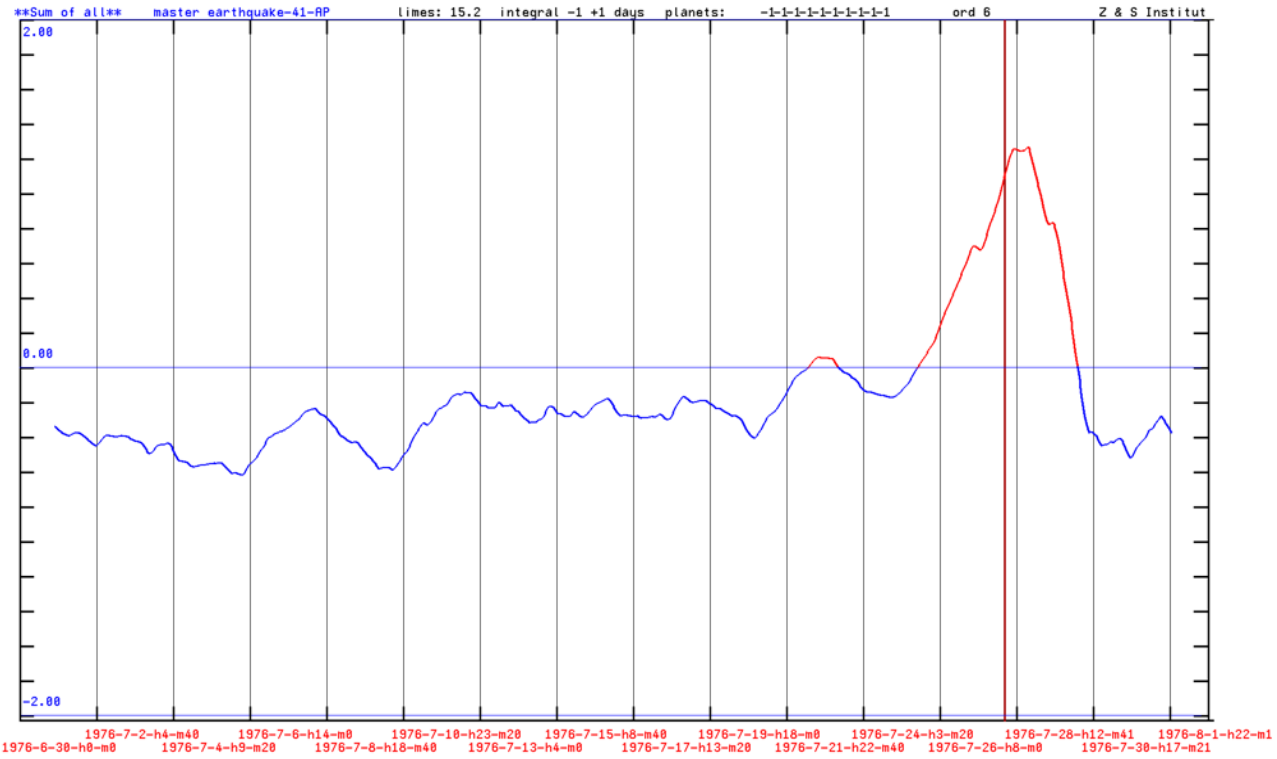

Figure 5. The month of the first earthquake (China; Tangshan; 28.7.1976; 03:42:00) from the list of 41 earthquakes. The time of the earthquake is indicated by the vertical red line. The curve indicates the change in the probability of an earthquake following the pattern of the 41 earthquakes. The sum over the pattern one day before the event to one day after the event was made here.

A list of earthquakes (Earthquakes of magnitude 6.5 or greater or those that caused fatalities, injuries or substantial damage. BRK-Berkeley. PAS-Pasadena.) in the time period [1997-01-05 to 2002-06-18], which contains major earthquakes in a relatively small time period, presents a particular challenge for pattern formation. A function that indicates a change for the probability of earthquakes must show the earthquakes from the list, but not very many from randomly selected events 513 earthquakes in 112 months, an average rate of 4.58 earthquakes per month.

Table 1 shows the process of optimization. First, only the matrix $H_{i,j}$ was optimized. The difference of earthquakes detected from the list of earthquakes to the continuum was 18%. The addition of other matrices reached a difference 49%. Table 1 clearly shows the influence of each matrix on the overall result. If all matrices are optimized simultaneously in the D4 space, the final result is 55% for the discriminatory power (difference).

82% from the group of 513 earthquakes were identified as earthquakes. From a randomly selected comparison group of 1000 events, 27% were identified as earthquakes. The comparison group of 1000 events was randomly selected over a period from 1900 to 2100. This 27% may include events where an earthquake has occurred or will occur.

Considering only the comparison period 1997 to 2002-6 in which the 513 earthquakes occurred, the pattern is: 52% are identified from the group of 513 earthquakes. 35% are identified as earthquakes from the comparison group of 1000 events. This results in a discriminatory power of only 17%.

The expected value that an event from the comparison group of 1000 randomly chosen events coincides with an earthquake from the group of 513 earthquakes is 255. Of the 1000 randomly chosen events for comparison, possibly about 255 events fall within ±12 h of an earthquake. This of course explains the low discriminatory power of 17%. The pattern should be valid beyond the period of the earthquake list, therefore the comparison period must be chosen larger.

In February 2023 (2023-02-06-01-17) a strong earthquake took place in areas of Turkey and Syria. Are these indicated by the two patterns 41 and 513 earthquakes? The study of earthquakes has shown that the time preceding the event is also characteristic. Therefore, the preceding day is also included in the following images.

Figure 5; Curve of the pattern 41 earthquake for the period 2023-2. The vertical red line marks the 2023-2-6-1-17 earthquake in Turkey and Syria.

From the curve (Figure 6) it cannot be seen that this earthquake was very probable. It does not fall under the recognized earthquakes. Probably here the stresses were so large that small events were already sufficient for triggering to occur.

The curve of pattern-513 (Figure 7) shows an area of increasing probability for an earthquake. The event thus falls into the group of earthquakes identified by the pattern.

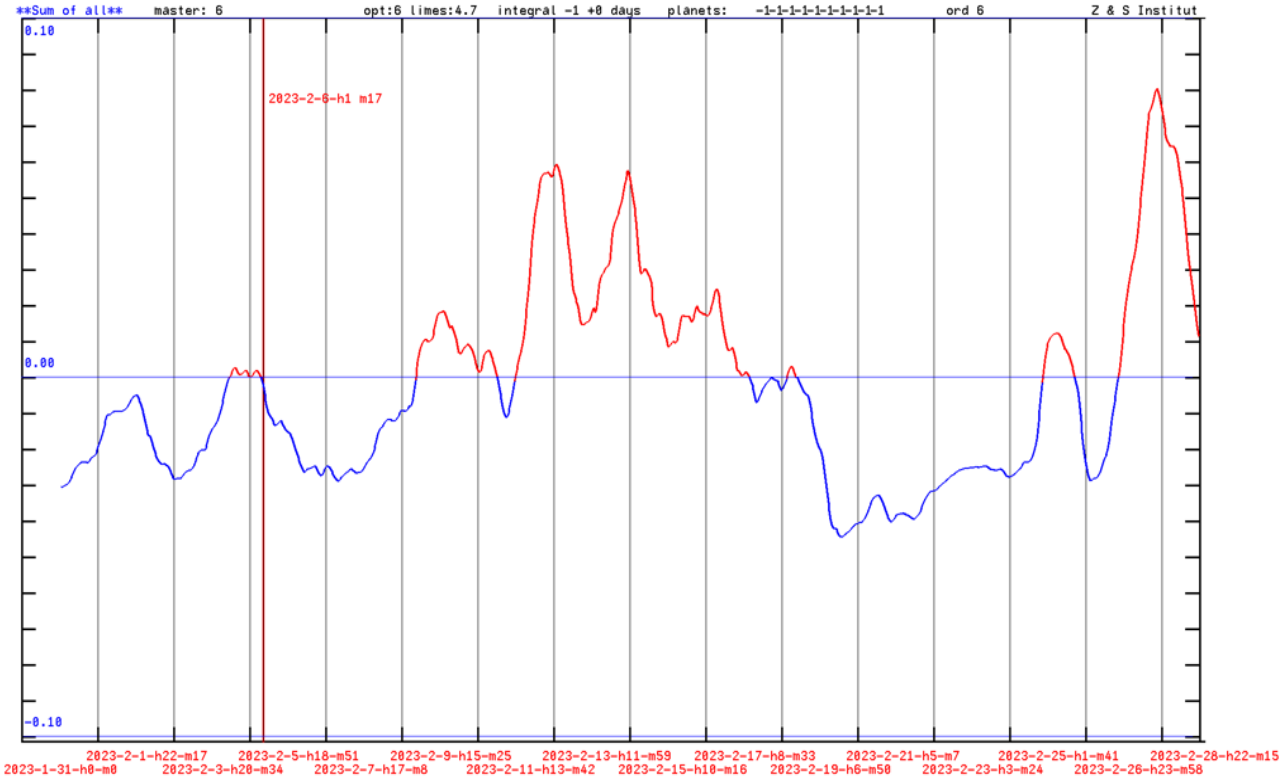

Figure 6. Curve of the pattern 41 earthquake for the period 2023-2. The vertical red line marks the 2023-2-6-1-17 earthquake in Turkey and Syria.

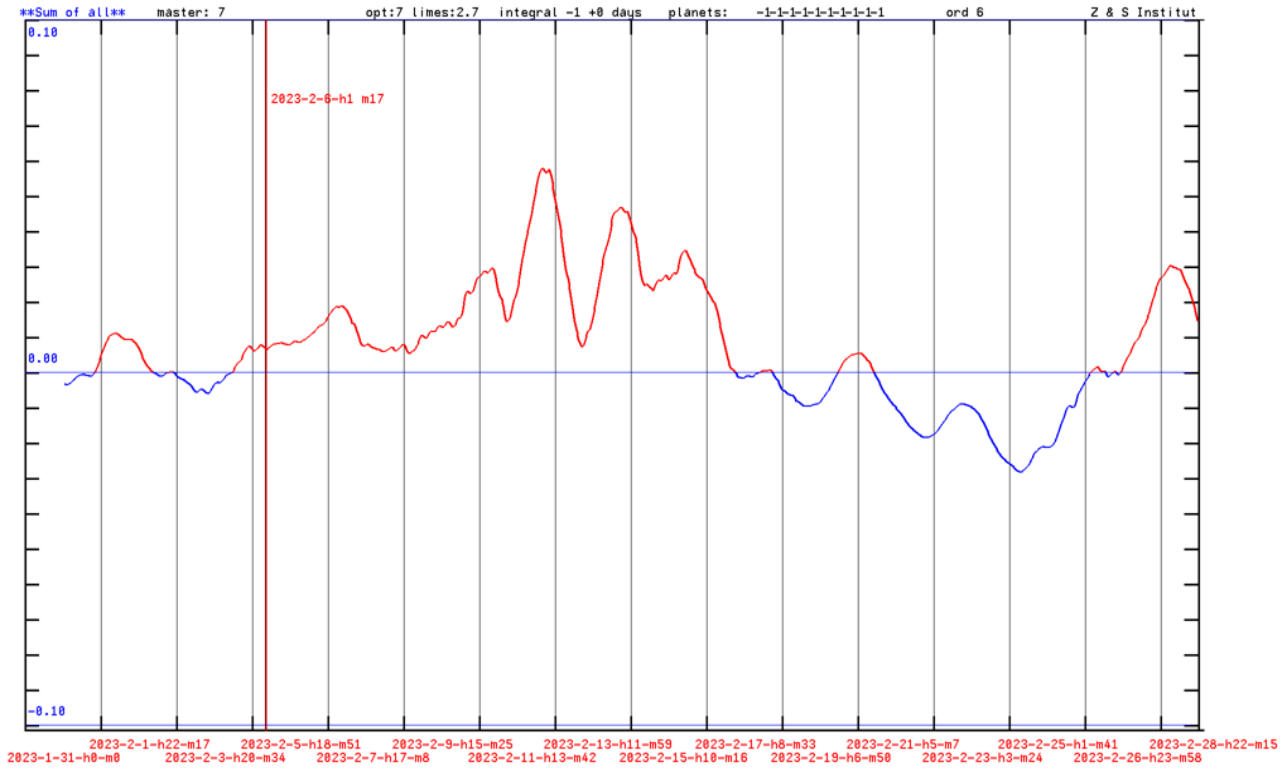

Figure 7. Curve of the pattern 513 earthquake for the period 2023-2. The vertical red line marks the earthquake 2023-2-6-1-17 in Turkey and Syria.

Table 1. The result of optimization: adding more matrices shows the improvement of the quality of the pattern (2).

Cumulation	Matrix *H*	+Matrix *D*	+Matrix *I*	+Matrix *DA*	all matrices
Difference/Sharpness Comparison period 1900 to 2100	18%	23%	45%	49%	55%

Although both patterns have recorded very different earthquakes, there is a very clear similarity in the curves. The 2023-2 period is well outside the time period in which the pattern-41 earthquakes (1900 to 2000 period) and 513 earthquakes (1997 to 2002-6 period) were produced.

2. Summary

The patterns studied here cannot predict earthquakes! However, they do indicate the increased probability of earthquakes from the oscillatory patterns of the planetary gravitational field. They are suitable, in the context of a larger AI, to be an element for probabilistic prediction of earthquakes. Other studies have also shown that Pluto need not be omitted, although its gravitational influence is certainly negligible. This is only plausible if one considers information, in addition to matter and energy, as a basic building block of the universe. The more or less strongly coupled oscillators (planets) in the solar system produce an oscillation pattern that represents a factor in the evolution [1].

Conflicts of Interest

The author declares no conflicts of interest regarding the publication of this paper.

References

[1] Nitsche, M.E. (2023) Fluktuations of the Planetary Gravitational Field and Nonlinear Interactions with Matter. Cuvillier Verlag, Göttingen.

[2] Nitsche, M. (2022) Triggering Earthquakes Fluctuations of the Planetary Gravitational Field and Nonlinear Interactions with Matter. *Earth & Environmental Science Research & Reviews*, **5**, 1-18. https://doi.org/10.33140/EESRR.05.01.08

[3] Brack, T., Zybach, B., Balabdaoui, F., *et al.* (2022) Dynamic Measurement of Gravitational Coupling between Resonating Beams in the Hertz Regime. *Nature Physics*, **18**, 952-957. https://doi.org/10.1038/s41567-022-01642-8

[4] Kennedy, *et al.* (2004) Earthquakes and the Moon: Syzygy Predictions Fail the Test. *Seismological Research Letters*, **75**, 607-612 https://doi.org/10.1785/gssrl.75.5.607

[5] Kasahara (2002) Tides, Earthquakes, and Volcanoes. *Science*, **297**, 348-349. https://doi.org/10.1126/science.1074601

[6] Metivier, *et al.* (2009) Evidence of Earthquake Triggering by the Solid Earth Tides. *Earth and Planetary Science Letters*, **278**, 370-375. https://doi.org/10.1016/j.epsl.2008.12.024

[7] Kolvankar, V.G. (2011) Sun, Moon and Earthquakes. *New Concepts in Global Tectonics Newsletter*.

https://www.academia.edu/30297793/Sun_Moon_and_Earthquakes

[8] Cochran, *et al.* (2004) Earth Tides Can Trigger Shallow Thrust Fault Earthquakes. *Science*, **306**, 1164-1166. https://doi.org/10.1126/science.1103961

[9] (1997) Tidal Phenomena. In: Wilhelm, H. and Wenzel, H.-G., Eds., *Lecture Notes in Earth Sciences*, 66, Vol. 66; Paperback - Illustrated, Springer, Berlin, 1st Edition.

[10] Nitsche, M. (2022) Fluctuations of the Planetary Gravitational Field and Nonlinear Interactions with Matter as an Element of Artificial Intelligence. *J Robot Auto Res*, **3**, 124-130.

[11] Nitsche, M. (2002) Are the Stabilizing and Destabilizing Influences of the Planetary Gravitational Field on the Structural Formation of Biological Patterns Real? *Lecture on the* 10*th Conference on Synergetics and Complexity Research*: "*Self Organization in Psychology*, *Psychiatry and Social Sciences*", Bavaria, 6-8 June 2002. http://www.planetare-korrelation.eu/index_htm_files/seon-2002-e.pdf

[12] Nitsche, M.E. (2001) The Non-Linear Interaction of the Planetary Gravitational Field on Earthquakes. *Lecture on the International Association for Mathematical Geology IAMG* 2003, Portsmouth, UK, 7-12 September 2003.

[13] (2003) EGS - AGU - EUG Joint Assembly. Abstracts from the Meeting, Nice, France, 6-11 April 2003. Abstract ID 1319.